Optical conductivity of the nonsuperconducting cuprate $La_{8-x}Sr_xCu_8O_{20}$

A. Lucarelli, S. Lupi, P. Calvani, and P. Maselli
Istituto Nazionale di Fisica della Materia, Dipartimento di Fisica, Università di Roma La Sapienza, Piazzale Aldo Moro 2, I-00185 Roma, Italy

G. De Marzi and P. Roy
Laboratoire pour l'Utilisation du Rayonnement Electromagnétique, Université Paris-Sud, 91405 Orsay, France

N. L. Saini and A. Bianconi
Istituto Nazionale di Fisica della Materia, Dipartimento di Fisica, Università di Roma La Sapienza, Piazzale Aldo Moro 2, I-00185 Roma, Italy

T. Ito and K. Oka
National Institute of Advanced Industrial Science and Technology, 1-1-1 Umezono, Tsukuba 305-8568, Japan
(Received 7 June 2001; published 9 January 2002)

$La_{8-x}Sr_xCu_8O_{20}$ is a nonsuperconducting cuprate which exhibits a doubling of the elementary cell along the *c* axis. Its optical conductivity has been first measured here, down to 20 K, in two single crystals with $x=1.56$ and $x=2.24$. Along *c*, bands are observed in both samples which correspond to strongly bound charges and confirm that the cell doubling is due to charge ordering. In the *ab* plane, in addition to the Drude term one observes an infrared peak at ~0.1 eV and a midinfrared band at 0.7 eV. The 0.1-eV peak is found at higher frequencies below 200 K, in correspondence with an anomalous increase in the dc resistivity and consistently with its assignment to localized charges. These results point out similarities and differences with respect to the optical properties of superconducting cuprates.

DOI: 10.1103/PhysRevB.65.054511 PACS number(s): 74.25.Gz, 71.38.−k, 78.30.−j

I. INTRODUCTION

In recent years, several studies have been devoted to the problem of localization and ordering of the doped charges in the cuprates. Theories of their metallic phase in terms of fluctuating charged stripes[1–4] have been proposed. Models of high-T_c superconductivity[5–7] have also been proposed, which assume a coexistence of free and bound charges. Experimentally, charged superlattices have been clearly detected by diffraction techniques in compounds[8] like $La_{2-x}Sr_xNiO_4$ or $La_{2-x}Sr_xMnO_4$, which are isostructural to $La_{2-x}Sr_xCuO_4$ (2-1-4). In this latter, however, ordered arrays of spin and charge have been observed only upon partial replacement of La by Nd.[9] On the other hand, charged stripe fluctuations have been detected in $YBaCu_3O_{7-x}$ by use of neutron scattering[10] and ion channeling[11] as well as, in 2-1-4, by x-ray absorption[12] and angle-resolved photoemission.[13]

As far as the optical spectra are concerned, it is well known that the complex optical conductivity $\sigma(\omega)$ of a metallic cuprate, measured in the *ab* plane, does not follow a normal Drude behavior. In the literature, this effect has been taken into account by using two different approaches. According to the so-called ''one component'' or ''anomalous-Drude'' model,[14,15] one assumes that both the carrier relaxation time τ and its effective mass m^* are functions of the photon frequency ω:

$$\tilde{\sigma}(\omega)=\frac{ne^2\tau(\omega)}{m^*(\omega)[1-i\omega\tau(\omega)]}. \tag{1}$$

This approach, which is most suitable to fit the smooth spectra of the HCTS close to optimum doping, has also been employed to extract from $\tilde{\sigma}(\omega)$ optical pseudogaps in a variety of cuprates.[15]

According to an alternative, multicomponent model, the real part of the infrared conductivity

$$\sigma(\omega)=\frac{\omega}{4\pi}\,\mathrm{Im}[\tilde{\epsilon}] \tag{2}$$

can be fitted by a Drude-Lorentz dielectric function

$$\tilde{\epsilon}=\epsilon_\infty-\frac{\omega_D^2}{\omega^2-i\omega\Gamma_D}+\sum_j\frac{S_j^2}{(\omega^2-\omega_j^2)-i\omega\Gamma_j}, \tag{3}$$

where, in the sum, one oscillator accounts for the so-called *d* band, another one for the midinfrared (MIR) band. Two further oscillators are often needed to reproduce the Cu-O charge-transfer band which appears in the near infrared and the visible.[17] The analysis of $\sigma(\omega)$ in terms of Eq. (3) is supported by the fact that the *d* and MIR contributions, which are needed to fit the spectra at optimum doping, have been directly resolved in a number of cuprates, both insulating and metallic.

The *d* band is observed at $\omega_d\sim0.1$ eV in both lightly doped La_2CuO_{4+y} (Ref. 18) and Nd_2CuO_{4-y} (Refs. 16 and 19) and is extremely sensitive to both doping and temperature. In $Nd_{2-x}Ce_xCuO_{4-y}$,[20] it increases in intensity and is displaced towards lower energies for both increasing doping and lowering temperatures.[20] The softening of an infrared band for $T\to0$ is quite unusual, as will be shown here also,

and allows one to make interesting comparisons with the nonsuperconducting oxides. The *d* contribution is still needed to fit $\sigma(\omega)$ at $x \simeq 0.15$, where $Nd_{2-x}Ce_xCuO_{4-y}$ is superconducting at optimum doping. Therein, it is found at frequencies even lower than the softest transverse phonon mode.[20,21] Finally, it disappears in the normal metallic phase at high doping ($x > 0.18$). Its presence in superconducting cuprates, at least those with low T_c, is confirmed by recent observations of superconducting $Bi_2Sr_2CuO_6$ close to optimum doping ($T_c = 20$ K).[22]

The above observations are explained by assuming that the *d* band is due to polaronic charges that increasingly self-trap at low *T* due to the competition between thermal excitations and charge-lattice interaction.[16,18,20,23,24] The softening of the charge binding energy for increasing polaron density (i.e., for increasing doping and/or decreasing temperature) is explained in terms of polaron-polaron interactions.[25–28] The strength of the *d* band seems also to increase as the dimensionality of the environment decreases. In $YBa_2Cu_4O_8$, an untwinned cuprate of the YBCO family that has both conducting Cu-O planes and Cu-O chains, the optical conductivity shows a Drude contribution well distinguished from a huge polaronic peak at 0.1 eV, when the radiation field is directed along the chains.[29] In turn, the nearly *T*-independent midinfrared band has been observed both in layered and cubic perovskites, upon doping, at ≈ 0.5 eV.[17,30,31] This band, which close to the MIT transition helps to build up the Drude term with part of its spectral weight,[17,30,31] is usually attributed to electronic states created by doping in the Cu-O charge-transfer gap.

In the present paper the optical properties of $La_{8-x}Sr_xCu_8O_{20}$ (8-8-20) will be studied and analyzed by using the model of Eq. (3). $La_{8-x}Sr_xCu_8O_{20}$ contains the same chemical species as the 40 K superconductor 2-1-4. However, (i) it is not superconducting for any *x*; (ii) it exhibits in the electron diffraction spectra well-defined superlattice spots for $x \sim 1.6$, indicating unit-cell doubling along the *c* axis, diffused spots for ~ 2.2.[32] Therefore, an infrared study of 8-8-20 can add information on the ordering process that takes place in this cuprate and provide interesting comparisons with the optical behavior of the superconducting cuprates.

II. SAMPLE DESCRIPTION AND EXPERIMENTAL PROCEDURE

The crystal structure of $La_{8-x}Sr_xCu_8O_{20}$ is tetragonal,[33] with lattice constants $a_0 = b_0 = 1.084$ nm, $c_0 = 0.3861$ nm. It can be derived from that of $La_{2-x}Sr_xCuO_4$ (2-1-4) by eliminating oxygen ions in a regular way. As a result, one is left with corner-sharing Cu-O_6 octahedra, Cu-O_5 pyramids, and Cu-O_4 squares. The latter ones form one-dimensional (1D) chains along the *c* axis, while the corner-sharing Cu-O_6 octahedra and the Cu-O_5 pyramids form a 3D network of essentially 1D paths. The charges travel along this network, and there are no Cu-O conducting sheets. The transport properties of $La_{8-x}Sr_xCu_8O_{20}$ have been investigated on single crystals with $1.56 < x < 2.24$. In this range the nominal charge varies from 0.2 to 0.3 holes per Cu atom, compared with from 0.06 to 0.3 holes per Cu atom in the metallic phase of $La_{2-x}Sr_xCuO_4$. Resistivity measurements on single crystals showed that 8-8-20, similarly to other cuprates, has an ''anomalous'' metallic region for $1.5 \lesssim x \lesssim 1.8$, followed by a normal metallic phase for $x \gtrsim 2$; however, for any *x*, it is not superconducting down to 1.3 K.[34] At room temperature the anisotropy in the resistivity is $\rho_c/\rho_{ab} \sim 10$ at any *x*. At constant temperature, both ρ_{ab} and ρ_c decrease for increasing *x*, as usually observed in doped Mott insulators. As a function of *T*, both ρ_{ab} and ρ_c are metallic like in the whole doping range, but exhibit an anomalous broad maximum[35] between two temperatures T_{c1} and T_{c2} (with $T_{c1} > T_{c2}$) which change with *x*. Here T_{c1} has been associated with a reduction in the scattering rate of the itinerant holes, related to a weak ferromagnetic ordering in the 3D network. Below T_{c2} an antiferromagnetic (AFM) order is observed and attributed to the chains of Cu-O_4 squares aligned along the *c* axis.[34] The AFM transition is associated with strong, opposite variations of the Hall coefficients R_H in the *ab* plane and along the *c* axis, and also with a sudden change in ρ_{ab}. These effects have been explained with the formation of a gap at the Fermi surface along certain directions, due to the formation of spin density waves at T_{c2}.[35] Both T_{c1} and T_{c2} decrease by increasing *x*, until a conventional metallic behavior is established in the sample with $x = 2.24$.[35] As already mentioned, electron diffraction studies[34] have shown that an ordering process causes a doubling of the elementary cell along the *c* direction. According to the authors, the ordering involves the charges introduced by doping, most probably in the CuO_4 squares. Indeed, one may remark that the anomalies in the resistivity of 8-8-20 are quite similar to those detected in compounds like $NbSe_3$, where one-dimensional charge density waves form below a critical temperature.[36]

The two single crystals selected for the present optical study of $La_{8-x}Sr_xCu_8O_{20}$ have $x = 2.24$ and $x = 1.56$, the highest and nearly the lowest doping level, respectively, which have been studied in the literature. Based on the transport properties[34] of crystals obtained from the same batch, the former should provide a good metallic spectrum for reference and the latter one, which has $T_{c1} = 145$ K and $T_{c2} = 85$ K, is expected to exhibit ''anomalous'' spectral features in the clearest way. Both crystals were grown by the traveling-solvent floating zone method.[35] Their chemical composition was determined by the inductively coupled plasma atomic emission (ICP-AES). The transport and magnetic properties of the samples have been described in Ref. 35.

The samples were mounted on the cold finger of a two-stage closed-cycle cryostat, whose temperature was kept constant within 2 K and could be varied from 295 to 20 K. The reflectance $R(\omega)$ of the samples, with the radiation field in the *ab* plane, was measured relative to gold- and aluminum-plated references. With the radiation field polarized along the *c* axis, the reference was obtained by evaporating directly gold on the sample.[37] Thus we obtained reliable absolute values of the reflectivity in spite of the small transverse dimension of the sample. The spectra were collected by a rapid scanning interferometer, typically from 80 to 20 000 cm^{-1}. A Drude-Lorentz fit was used to extrapolate the reflectivity to

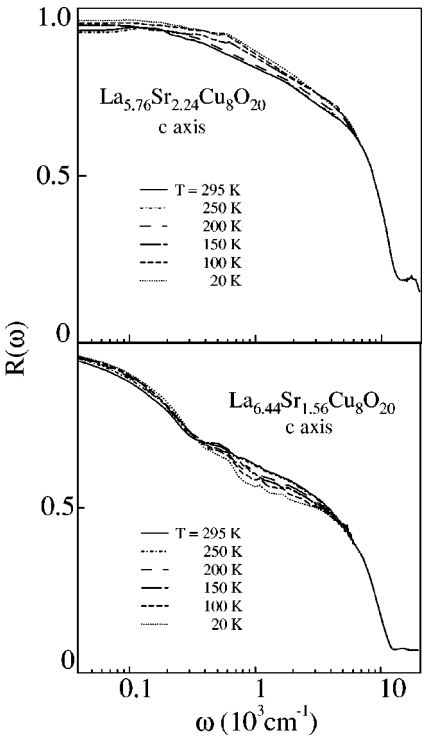

FIG. 1. Infrared reflectivity measured up to 20 000 cm^{-1} at different temperatures, with the radiation field polarized along the *c* axis for both $x=2.24$ (top) and $x=1.56$ (bottom).

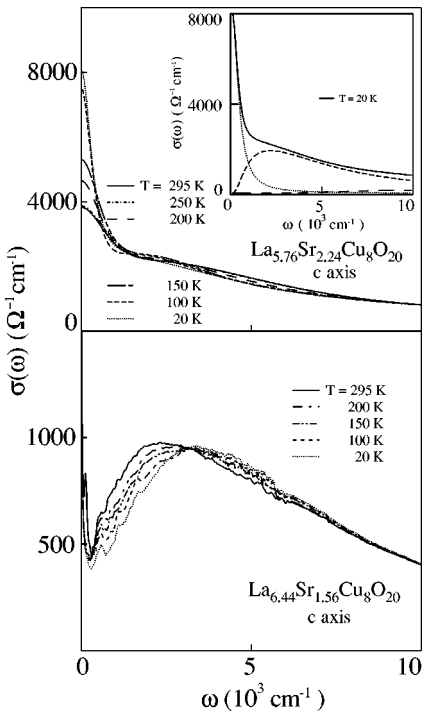

FIG. 2. Infrared optical conductivity of the *c* axis at different temperatures, as extracted from the $R(\omega)$ of Fig. 1, for $x=2.24$ (top) and $x=1.56$ (bottom). The inset compares the experimental $\sigma(\omega)$ at 20 K (solid line) with a fit based on a conventional Drude term (dotted line) and two contributions at infrared frequencies (dashed lines).

$\omega=0$. On the high-energy side, our data were extrapolated with the reflectivity reported in Ref. 38 for $La_{2-x}Sr_xCuO_4$, under the reasonable assumption that the ultraviolet bands of 8-8-20 are not too different from those of 2-1-4. The real part of the optical conductivity $\sigma(\omega)$ was then extracted from $R(\omega)$ by usual Kramers-Kronig transformations.

III. RESULTS AND DISCUSSION

A. Optical response of the *c* axis

The reflectivity $R(\omega)$ measured along the *c* axis of $La_{8-x}Sr_xCu_8O_{20}$ is shown in Fig. 1 for $x=2.24$ (top) and $x=1.56$ (bottom). The spectra are reported in the range from 40 to 20 000 cm^{-1} at six different temperatures. $R(\omega)$ exhibits a metalliclike behavior in both samples with a well-evident pseudoplasma edge around 10 000 cm^{-1}. The electronic band in the visible range is similar to features observed in most cuprates.[17,30] and attributed to the Cu-O charge-transfer transitions. For $x=2.24$, it can be reproduced by two Lorentzians placed at 17 800 and 21 200 cm^{-1}, with $\epsilon_\infty=4.1$. At low frequency $R(\omega)$ differs in the two crystals. The sample with $x=2.24$ shows a standard metallic reflectivity, except for a smooth anomaly at $\sim$600 cm^{-1} for $T \lesssim 150$ K. On the other hand, for $x=1.56$ there is a clear change of slope in $R(\omega)$ around 300 cm^{-1}, suggestive of two different contributions to $\sigma(\omega)$. The contribution at high frequency exhibits a more pronounced temperature dependence than that at low frequency.

The multicomponent structure of the absorption is evident in the real part of the optical conductivity, reported for both crystals in Fig. 2. In the sample with $x=2.24$ (top), $\sigma(\omega)$ exhibits two well-defined components in the infrared, with different temperature behaviors: a Drude term which is dominating for $\omega \lesssim 1500\ cm^{-1}$ and narrows for $T \to 0$ and a broadband in the midinfrared. This latter is separated from the Drude contribution by a change of slope at $\sim$1500 cm^{-1}, more pronounced at low *T*. The inset compares the experimental $\sigma(\omega)$ at 20 K with a fit to Eq. (3). In the frequency range shown in the inset, this includes a Drude term with $\omega_p \simeq 1500\ cm^{-1}$ at all temperatures and a Γ_D which decreases from 1200 cm^{-1} at 295 K to 400 cm^{-1} at 20 K, a contribution in the midinfrared peaked at 2300 cm^{-1} at 20 K and a weak background centered at about 9000 cm^{-1}. Based on these results, it seems quite reasonable to assign the midinfrared band to those bound charges which produce a diffuse scattering in the electron diffraction spectra of the $x=2.2.4$ sample. In turn, the strong Drude term accounts for the good dc conductivity of this compound along the *c* axis. Therefore the present data show a coexistence of free and bound charges in the cuprate even at $x=2.24$, a doping value which provides at all temperatures the lowest dc resistivity reached by this compound.

A Drude-like absorption and a band in the midinfrared are found also in the sample with $x=1.56$ (bottom panel of Fig. 2) where, however, they are directly resolved in the $\sigma(\omega)$. This is due to the fact that the Drude term is weaker than at $x=2.24$ by a factor of 10, the midinfrared band by a factor of 2. By recalling the results of Ref. 35, one may assign the

sharp, *T*-dependent midinfrared band here observed for $x=1.56$ to the photoexcitation of those bound charges which, for $x=1.6$, contribute sharp superlattice spots to the electron diffraction spectra. The peak frequency increases monotonically from $\sim 2300\ \mathrm{cm}^{-1}$ at 295 K to $\sim 3300\ \mathrm{cm}^{-1}$ at 20 K. At the latter temperature, the corresponding band in the inset of Fig. 2 is peaked at $\sim 2000\ \mathrm{cm}^{-1}$. As already mentioned, a softening of the bound-charge absorption for increasing doping has also been observed in superconducting families of cuprates.[20] If one describes the bound charges in terms of small polarons, as previously done for other perovskites with charge ordering,[39,40] the peak energy of the band is just twice the charge-lattice binding energy E_p.[41] From Fig. 2, at $x=1.56$ one thus finds $E_p \sim 1100\ \mathrm{cm}^{-1}$ at 295 K, $E_p \sim 1600\ \mathrm{cm}^{-1}$ at 20 K.

The full opening of a charge-ordering gap in $\sigma(\omega)$, as observed, for instance,[40] in $La_{1.67}Sr_{0.33}NiO_4$, is prevented in $La_{6.44}Sr_{1.56}Cu_8O_{20}$ by the Drude-like component, which in Fig. 2 is observed at any temperature. This shows that the bound charges are coexisting with free charges in the 1.56 crystal, consistently with its not negligible dc conductivity. Due to the peculiar structure of 8-8-20 along the *c* axis, the two types of charges are likely to be even spatially separated. The ordered charges can occupy the CuO_4 chains, as already proposed,[34] while the free carriers may travel along the zigzag paths formed by the polyhedrical network, which are aligned in average along the *c* direction. A similar situation is encountered, for instance, in $NbSe_3$, which remains metallic down to the lowest temperatures in spite of the formation of charge density waves. These latter appear in two out of the three infinite-length trigonal prisms that build up the structure of $NbSe_3$, while the third one remains metallic.[42]

B. Optical response of the *ab* plane

The reflectivity $R(\omega)$ of the *ab* plane of $La_{8-x}Sr_xCu_8O_{20}$ is shown in Fig. 3 for $x=2.24$ (top) and $x=1.56$ (bottom). The spectra are reported in the range from 80 to 3000 cm^{-1} at different temperatures. In the insets of both figures $R(\omega)$ is shown at two temperatures in the energy range from 80 to 20 000 cm^{-1}. Here $R(\omega)$ presents a metalliclike behavior in both samples with a well-evident pseudoplasma edge around 10 000 cm^{-1}. However, below 3000 cm^{-1} the reflectivity of the sample with $x=2.24$ (top panel) increases steadily by lowering the temperature according to a conventional metallic behavior, while in the sample with $x=1.56$ (bottom panel) $R(\omega)$ has a more complicated behavior. Indeed, by lowering *T* the reflectivity first increases down to 250 K; then, it decreases to reach at 20 K its minimum value.

The real part $\sigma(\omega)$ of the optical conductivity is shown in Fig. 4 for both samples, between 80 and 5000 cm^{-1} and at different temperatures. In the sample with $x=2.24$ (top panel) $\sigma(\omega)$ exhibits a pronounced metallic behavior. However, the behavior $\sigma(\omega) \propto \omega^{-1}$ that is observed in other cuprates and that inspired the ''anomalous Drude'' model of Eq. (1) is not observed here. On the other hand, a best fit to Eq. (3) gives very good results (see the inset, where the fit is superimposed to data) by using a normal Drude term plus a nearly flat background. This latter, in turn, is obtained by a

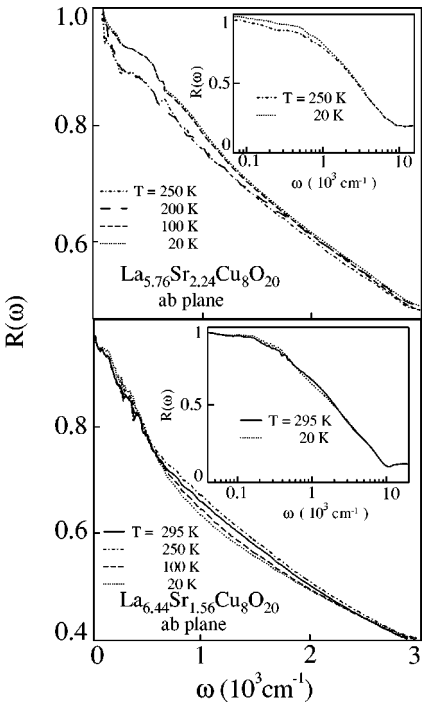

FIG. 3. Infrared reflectivity measured at different temperatures, with the radiation field polarized in the *ab* plane for both $x=2.24$ (top) and $x=1.56$ (bottom). In the insets, $R(\omega)$ is shown at two temperatures up to 20 000 cm^{-1}.

superposition of Lorentzians peaked in the midinfrared (2500 cm^{-1}) and in the visible. The Drude plasma frequency ($\omega_D \sim 5500\ \mathrm{cm}^{-1}$) is approximately independent of temperature, while Γ_D decreases from 250 cm^{-1} at 295 K to 90 cm^{-1} at 20 K. By using these values one predicts a $\sigma_{\mathrm{dc}} = \omega_D^2/[60\Gamma_D] \sim 6000$ (2000) $\Omega^{-1}\,\mathrm{cm}^{-1}$ at 20 K (250 K) for the $x=2.24$ sample, in agreement with the measured values[35] within a factor of 2.

In the sample with $x=1.56$ (bottom panel), where the anomalies in the dc properties are most evident, $\sigma(\omega)$ exhibits a complex structure. In the inset, $\sigma(\omega)$ is shown at two temperatures in the whole energy range. At least four absorption bands are directly observed in the spectrum, which then suggests a fit in terms of the Drude-Lorentz approach. The band at the highest energy is a broad absorption located around 15 000 cm^{-1}, independent of *T*, which may be assigned to the charge-transfer transition between Cu and O. A second well-evident absorption is observed around 6000 cm^{-1} and is nearly independent of temperature. This feature is then different from the midinfrared bands observed along the *c* axis and assigned to bound charges. It is instead similar to the midinfrared band observed in most HCTS.[30,17] According to a pseudopotential calculation[43] of the electronic structure of $La_4BaCu_5O_{13}$, a compound with lattice structure and transport properties similar to those of $La_{8-x}Sr_xCu_8O_{20}$, the MIR band is due to a transition from an electronic band located at ~ 0.5 eV below the Fermi energy E_F to a band which crosses E_F.

A third absorption in the bottom panel of Fig. 4 is strongly dependent on *T* and extends from ~ 500 to $\sim 4000\ \mathrm{cm}^{-1}$. Let us name its peak frequency ω_d, for its similarity with other

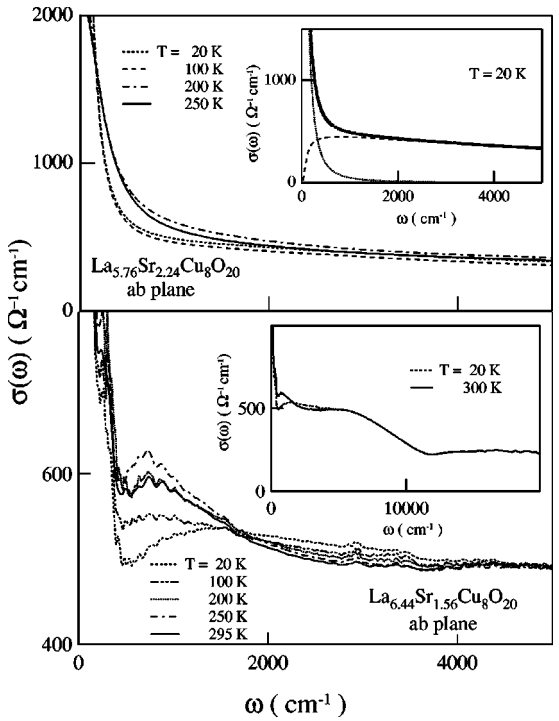

FIG. 4. Infrared optical conductivity in the *ab* plane for the two crystals, as extracted from the $R(\omega)$ of Fig. 3 at different temperatures. In the upper inset, the experimental $\sigma(\omega)$ for $x=2.24$ is shown at 20 K (thick dots) together with a fit (solid line) given by a Drude term (dotted line) plus a broad background reproduced by a sum of Lorentzians (dashed line). In the lower inset, $\sigma(\omega)$ is shown for the $x=1.56$ crystal in the whole measuring range.

cuprates mentioned in the Introduction, where the corresponding band is assigned to the photoexcitation of polaronic charges.[18,20,24,29] At low temperature the *d* peak is separated from the *T*-independent MIR band by a broad minimum centered at about 3000 cm^{-1} (see also the inset). Another minimum at lower frequency, between this third absorption and the Drude term, deepens for decreasing temperature and recalls the optical pseudogaps reported for several underdoped cuprates.[15] However, one sees from Fig. 4 that such deepening is due to a ''blueshift'' of the *d* band. Indeed, in the present $La_{6.64}Sr_{1.56}Cu_8O_{20}$ crystal ω_d remains constant at $\sim$800 cm^{-1} between 295 and 200 K, but at lower temperatures it *hardens* to reach about 1500 cm^{-1} at 20 K. This behavior with temperature is quite different from that of superconducting cuprates, where usually ω_d *softens* for $T\rightarrow 0$. The intensity of the *d* peak increases from 295 to 250 K to decrease gradually from 250 to 20 K.

One can easily check that the displacement of the *d* band occurs via a transfer of spectral weight within the low-energy excitation spectrum of the carriers. Indeed, as one can see in the bottom panel of Fig. 4, $\sigma(\omega)$ is independent of *T* both at about 1700 cm^{-1} and at 5000 cm^{-1}. If one introduces the effective number of carriers

$$\eta_{\rm eff}(\omega_1,\omega_2)=\frac{2m^*V}{\pi e^2}\int_{\omega_1}^{\omega_2}\sigma(\omega)d\omega. \qquad (4)$$

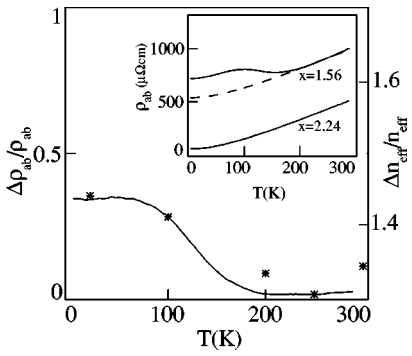

FIG. 5. Behavior with temperature of the infrared spectral weight of $La_{6.44}Sr_{1.56}Cu_8O_{20}$ in the *ab* plane, compared with that of its dc resistivity, ρ_{ab}. Raw ρ_{ab} data are reported in the inset for both $x=1,56$ and $x=2.24$ as solid lines. The dashed line is the ρ_{ab} of $x=2.24$, assumed as a normal metallic reference, once scaled by a constant factor in order to match the high-*T* ρ_{ab} of $x=1.56$. In the main figure, the solid line gives $\Delta\rho_{ab}/\rho_{ab}=[\rho_{ab}(1.56)-\rho_{ab}(2.24)]/\rho_{ab}(2.24)$: namely, the deviation of ρ_{ab} in the $x=1.56$ sample from a normal metallic behavior. The stars represent the ratio $\Delta n_{\rm eff}/n_{\rm eff}=[n_{\rm eff}(80,5000)-n_{\rm eff}(80,1700)]/n_{\rm eff}(80,1700)$ as obtained from the $\sigma(\omega)$ of Fig. 4 through Eq. (4).

where *V* is the cell volume and m^* is assumed to be equal to the free-electron mass, and puts $\omega_1=80\,cm^{-1}$, $\omega_2=5000\,cm^{-1}$, one obtains $n_{\rm eff}(80,5000)=1.15\pm0.02$ at any *T* from 295 to 20 K. Therefore, as *T* changes, spectral weight is transferred across the fixed point at 1700 cm^{-1} with no intervention from the electronic transitions at higher energies. This transfer is measured by the ratio $\Delta n_{\rm eff}/n_{\rm eff}=[n_{\rm eff}(80,5000)-n_{\rm eff}](80,1700)]/n_{\rm eff}(80,1700)$, which is reported at five temperatures in Fig. 5. One should notice that the error in this quantity is on the order of 2%. Therein, $\Delta n_{\rm eff}/n_{\rm eff}$ is also compared with the behavior of dc resistivity in the same sample. Indeed, in the inset of the figure, the *ab*-plane raw resistivity ρ_{ab} is reported by a solid line for both crystals here considered.[35] Due to the reduced number of carriers, at $x=1.56$, ρ_{ab} is larger than for the $x=2.24$ sample, which behaves approximately like a conventional metal. However, if one scales ρ_{ab} for this latter by a constant factor (dashed line), the two curves show the same temperature dependence between 295 and 200 K. On the other hand, below 200 K, ρ_{ab} for $x=1.56$ deviates significantly upwards from its behavior at $x=2.24$. In the main figure, the solid line $\Delta\rho_{ab}/\rho_{ab}=[\rho_{ab}(1.56)-\rho_{ab}(2.24)]/\rho_{ab}(2.24)$ measures such a deviation. As one can see, this line qualitatively follows the transfer of infrared spectral weight towards higher frequencies as *T* is lowered, indicated by $\Delta n_{\rm eff}/n_{\rm eff}$ (stars). Therefore, one finds that the variation in the dc resistivity is related to the ''blueshift'' of an infrared oscillator at finite frequency, well distinguished from the Drude term, the so-called *d* band. This observation is consistent with the assignment of the *d* band in this cuprate to self-trapped charges. Indeed, according to any polaronic model of $\sigma(\omega)$,[41] $\omega_d\propto E_p$, the self-trapping energy of the carrier. Therefore, in this framework the observed hardening of the *d* band below 200 K implies a lower hopping rate of the carriers, consistent with the anomalous increase observed below 200 K in the dc resistivity.

Finally, below 500 cm^{-1} the *ab*-plane infrared conductivity of both samples in Fig. 4 shows a Drude-like free-particle absorption. Phononlike peaks are superimposed onto it, more clearly for $x=1.56$ due to a reduced screening effect of the carriers. The extrapolations of $\sigma(\omega)$ to $\omega=0$ at different temperatures agree within a factor of 2 with the corresponding values of σ_{dc} extracted from the resistivities of Fig. 4.

IV. CONCLUSION

We have studied the optical properties of $La_{8-x}Sr_xCu_8O_{20}$, a nonsuperconducting cuprate characterized by a network of essentially one-dimensional paths. The two single crystals here examined have $x=1.56$ and $x=2.24$ or, approximately, the lowest and highest dopings, respectively, that have been studied in the literature for this compound.

We have first determined the optical response of the *c* axis, where previous electron diffraction experiments on $La_{8-x}Sr_xCu_8O_{20}$ showed clear superlattice spots for $x=1.6$, diffuse superlattice scattering for $x=2.24$. In the optical spectra, for $x=1.56$ we find a strong and *T*-dependent midinfrared band accompanied by a weak Drude term. At $x=2.24$ we observe a broad, nearly *T*-independent, midinfrared background coexisting with a strong and narrow Drude term. The observation of such infrared features confirms that the cell doubling along the *c* axis is due to charge ordering. Midinfrared bands similar to those reported here have been observed in other oxides (like nickelates and manganites) which exhibit either commensurate or incommensurate ordering. Therein, however, the Drude term is usually absent below the ordering temperature. In the present cuprate, on the contrary, the ordered charges coexist with carriers moving freely along the *c* axis, because the two species are probably placed on different paths. In any case, once again the observation of a *T*-dependent midinfrared absorption in a cuprate is intimately related to selftrapped, or polaronic, charges, which at high doping may form ordered structures.

We have then studied the *ab* plane of $La_{8-x}Sr_xCu_8O_{20}$, where no indications of superlattice features are extracted from the diffraction experiments. The infrared spectra of the $x=1.56$ crystal exhibit again both a Drude-like term and a well-resolved midinfrared absorption. However, the latter band is much softer than for the *c* axis of the same sample ($\sim$0.1 eV with respect to 0.3 eV). A fit to the $x=2.24$ optical conductivity confirms the above two-term scenario also for the highest doping. However, unlike along the *c* axis, in the *ab* plane one could have a single type of lightly bound carriers, possibly large polarons. The Drude part of the spectrum would reflect their behavior as quasifree particles; the soft band at 0.1 eV would correspond to their photoionization: i.e., their destruction by absorption of a photon. This interpretation is consistent with the observed correlation between the *T* dependence of the band at 0.1 eV and that of the dc resistivity in the same $x=1.56$ sample.

By recalling what reported in the Introduction, the *ab* plane of $La_{8-x}Sr_xCu_8O_{20}$ behaves in the infrared like the *ab* plane of the superconducting cuprates, even if it has a quite different geometrical structure. However, a crucial difference has been pointed out by the present experiment. While in the nonsuperconducting 8-8-20 the infrared bands related to the bound charges move to higher frequencies for $T\rightarrow 0$, indicating stronger localization, in some high-T_c superconductors the corresponding absorption is found to soften for decreasing temperature in the normal phase, indicating a carrier delocalization or—in a phase separation scenario—stronger charge density fluctuations. This result should be taken into consideration by those models where the existence of bound charges is related to the still unexplained phenomenon of high-T_c superconductivity.

ACKNOWLEDGMENTS

We are indebted to M. Capizzi and P. Quemerais for useful discussions and suggestions.

[1] V. J. Emery and S. A. Kivelson, Physica C **209**, 597 (1993); Phys. Rev. Lett. **71**, 3701 (1993).
[2] C. Castellani, C. Di Castro, and M. Grilli, Phys. Rev. Lett. **75**, 4650 (1995).
[3] M. I. Salkola, V. J. Emery, and S. A. Kivelson, Phys. Rev. Lett. **77**, 155 (1996).
[4] A. Sadori and M. Grilli, Phys. Rev. Lett. **84**, 5375 (2000).
[5] J. Ranninger, Solid State Commun. **85**, 929 (1993); J. Ranninger, J. M. Robin, and M. Eschrig, Phys. Rev. Lett. **74**, 4027 (1995).
[6] A. Bianconi, A. Valletta, A. Perali, and N. L. Saini, Solid State Commun. **102**, 369 (1997).
[7] P. Quemerais and S. Fratini, Physica C **341,** 229 (2000).
[8] C. H. Chen and S.-W. Cheong, Phys. Rev. Lett. **76**, 4042 (1996); W. Bao, S-W. Cheong, and W. Chen, Solid State Commun. **98**, 55 (1996).
[9] J. M. Tranquada, B. J. Sternlieb, J. D. Axe, Y. Nakamura, and S. Uchida, Nature (London) **375**, 561 (1995).
[10] H. A. Mook, P. Dai, F. Dogan, and R. D. Hunt, Nature (London) **404**, 729 (2000).
[11] R. P. Sharma, S. B. Ogale, Z. H. Chang, J. R. Liu, W. K. Chu, B. Veal, A. Paulikas, H. Zheng, and T. Venkatesan, Nature (London) **404**, 736 (2000).
[12] A. Bianconi, N. L. Saini, A. Lanzara, M. Missori, T. Rossetti, H. Oyanagi, H. Yamaguchi, K. Oka, and T. Ito, Phys. Rev. Lett. **76**, 3412 (1996).
[13] A. Ino, C. Kim, M. Nakamura, T. Yoshida, T. Mizokawa, Z.-X. Shen, A. Fujimori, T. Kakeshita, H. Eisaki, and S. Uchida, cond-mat/9902048 (unpublished).
[14] Z. Schlesinger, R. T. Collins, F. Holtzberg, C. Feild, G. Koren, and A. Gupta, Phys. Rev. B **41**, 11 237 (1990).
[15] T. Timusk and B. Statt, Rep. Prog. Phys. **62**, 61 (1999).
[16] P. Calvani, M. Capizzi, S. Lupi, P. Maselli, A. Paolone, and P. Roy, Phys. Rev. B **53**, 2756 (1996).
[17] S. Lupi, P. Calvani, M. Capizzi, P. Maselli, W. Sadowski, and E.

Walker, Phys. Rev. B **45**, 12 470 (1992).
[18] J. P. Falck, A. Levy, M. A. Kastner, and R. J. Birgenau, Phys. Rev. B **48**, 4043 (1993).
[19] G. A. Thomas, D. A. Rapkine, S-W. Cheong, and L. F. Schneemeyer, Phys. Rev. B **47**, 11 369 (1993).
[20] S. Lupi, P. Maselli, M. Capizzi, P. Calvani, P. Giura, and P. Roy, Phys. Rev. Lett. **83**, 4852 (1999).
[21] E. J. Singley, D. N. Basov, K. Kurahaschi, T. Uefuji, and K. Yamada, cond-mat/0103480 (unpublished).
[22] S. Lupi, P. Calvani, M. Capizzi, and P. Roy, Phys. Rev. B **62**, 12 418 (2000).
[23] Y. Yagil and E. K. H. Salje, Physica C **256**, 205 (1996).
[24] R. P. S. M. Lobo, F. Gervais, and S. B. Oseroff, Europhys. Lett. **37**, 341 (1997).
[25] S. Fratini and P. Quemerais, Mod. Phys. Lett. B **12**, 1003 (1998); Eur. Phys. J. (to be published).
[26] V. Cataudella, G. De Filippis, and G. Iadonisi, Eur. Phys. J. B **12**, 17 (1999).
[27] J. Tempere and J. T. Devreese, Phys. Rev. B **64,** 104504 (2001).
[28] J. Tempere and J. T. Devreese, Eur. Phys. J. B **20,** 27 (2001).
[29] B. Bucher, J. Karpinski, E. Kaldis, and P. Wachter, Phys. Rev. B **45**, 3026 (1992).
[30] S. Uchida, H. Takagi, and Y. Tokura, Physica C **162–164**, 1677 (1989).
[31] S. H. Blanton, R. T. Collins, K. H. Kelleher, L. D. Rotter, Z. Schlesinger, D. G. Hinks, and Y. Zheng, Phys. Rev. B **47**, 996 (1993).
[32] H. Yamaguchi, H. Matsuhata, T. Ito, and K. Oka, Physica C **282–287**, 1079 (1997).
[33] L. Er-Rakho, C. Michel, and B. Raveau, J. Solid State Chem. **73**, 514 (1988).
[34] T. Ito, H. Yamaguchi, K. Oka, K. Nozawa, and H. Takagi, Phys. Rev. B **60**, R15 031 (1999).
[35] T. Ito, H. Yamaguchi, and K. Oka, Chin. J. Low Temp. Phys. **19**, 36 (1997).
[36] J. Chaussy, P. Haen, J. C. Lasjaunias, P. Monceau, G. Waysand, A. Waintal, A. Meerschaut, P. Molinie, and J. Rouxel, Solid State Commun. **20**, 759 (1976).
[37] C. C. Homes, M. Reedik, D. A. Cradles, and T. Timusk, Appl. Opt. **32**, 2976 (1993).
[38] S. Tajima, H. Ishi, T. Nakahashi, T. Takagi, S. Uchida, M. Seki, S. Suga, Y. Hialaka, M. Suzuki, T. Murakami, K. Oka, and H. Unoki, J. Opt. Soc. Am. B **6**, 475 (1989).
[39] X. Bi and P. C. Eklund, Phys. Rev. Lett. **70**, 2625 (1993); Phys. Rev. B **48**, 4043 (1993).
[40] P. Calvani, A. Paolone, P. Dore, S. Lupi, P. Maselli, P. G. Medaglia, and S-W. Cheong, Phys. Rev. B **54**, R9592 (1996).
[41] D. Emin, Phys. Rev. B **48**, 13 691 (1993).
[42] P. Monceau, *Electronic Properties of Inorganic Quasi-One-Dimensional Compounds* Part II, D. (Reidel, Dordrech, 1985), Pt. II. pp. 139–268.
[43] F. Hermann, R. V. Kasowski, and W. Hsu, Phys. Rev. B **37**, 2309 (1998).